ICCV-5, 1995, 434-439

A Geometric Criterion for Shape-based Non-rigid Correspondence

Hemant D. Tagare
Dept. of Diagnostic Radiology
Dept. of Computer Science
Yale University
New Haven, CT 06520

Donal O'Shea
Dept. of Mathematics
Mt. Holyoke College
South Hadley, MA 01075

Anand Rangarajan
Dept. of Diagnostic Radiology
Dept. of Computer Science
Yale University
New Haven, CT 06520

Abstract

A geometric criterion is developed for establishing shape-based non-rigid correspondence between plane curves. Unlike previous efforts, the criterion does not use rigid invariants of shape. Instead, shapes are compared non-rigidly from the vantage point of the correspondence.

Geometric invariants are proposed for curves whose shapes can be exactly matched by a non-rigid correspondence. The invariants are based on angular deviations of convex and concave segments of the curves.

Examples of correspondences between curves obtained from medical images are provided.

1 Introduction

Analysis of medical images often requires a correspondence between a pair of closed curves. An optimal correspondence is obtained by choosing a set of admissible correspondences and a preference relation amongst its elements.

Correspondences in medical applications are usually continuous and non-rigid, with the most desirable correspondence optimally aligning the local shapes of the two curves.

Previous algorithms model non-rigid correspondence as differentiable functions from one curve to another, and the preference between different correspondences is based on similarity of numerical values of curvature at corresponding points. This approach has two drawbacks: (1) Curvature is a rigid invariant of shape and its applicability to non-rigid correspondence is problematic, (2) Since the set of differentiable functions from a curve to another is not the same as the set of differentiable functions in the reverse direction, the optimal correspondence from curve C_1 to curve C_2 is not guaranteed to be the same as the optimal correspondence from C_2 to C_1.

The algorithm proposed in this paper overcomes these problems. It uses a criterion for shape comparison that does not rely on rigid invariants, and it uses a "symmetric" space of correspondences so that the optimal correspondence from C_1 to C_2 is the same as that from C_2 to C_1.

The space of correspondences is defined in section 2. The geometric criterion for non-rigid comparison of shapes is proposed in section 3. The numerical algorithm for computing the optimal correspondence is described in section 5. Experiments are included in section 6.

The geometric criterion also gives equivalence classes of curves. We pursue this in section 4.

Lack of space forces us to omit proofs of the theoretical results of the paper. They will be available in a forthcoming report [9].

1.1 Previous Work

Shape based non-rigid correspondence has been investigated in [1][3][7], where the correspondence is obtained by minimizing differences in curvature at corresponding points. As mentioned before, the applicability of curvature to non-rigid cases is problematic.

Correspondence between curves can also be viewed as the restriction to the curves of a mapping from the image containing the first curve to the image containing the second. Prior knowledge about the mapping can impose constraints on the correspondence [5][6].

A different but related problem is that of non-rigid registration [8]. Here, an image transformation is sought which maps an embedded curve in one image close to an embedded curve in another. Registration differs from correspondence in that points of the first curve need not fall on the second curve. They need only be near the second curve in its image space. Registration need not give correspondence.

2 Correspondence and Topology

If C_1 and C_2 are two oriented plane curves, then the product space $C_1 \times C_2$ is the space of ordered pairs (u, v) of all $u \in C_1$ and all $v \in C_2$. For any element $(u, v) \in C_1 \times C_2$, the projection operator $p_1 : C_1 \times C_2 \rightarrow C_1$ gives the first component of the ordered pair, $p_1((u, v)) = u$; and the projection operator $p_2 : C_1 \times C_2 \rightarrow C_2$ gives the second component, $p_2((u, v)) = v$.

Correspondence is a set of ordered pairs of points of two curves. It is naturally defined as a subset of the product space of the curves.

A *correspondence* Φ is a subset of $C_1 \times C_2$ whose projections on C_1 and C_2 are onto. We say that an element μ of Φ *pairs* the point $p_1(\mu)$ in C_1 with the point $p_2(\mu)$ in C_2. The space of all correspondences is too big to be of use in medical applications. We consider two smaller classes of correspondences.

A *diffeomorphic correspondence* is a one-to-one correspondence which can be expressed as a diffeomorphism (a one-to-one function with a differentiable inverse) from the arc-length of C_1 to the arc length of C_2, i.e., if s_1 is the arc-length of C_1 and s_2 is the arc length of C_2, then $\Phi = \{(C_1(s_1), C_2(s_2))\}$ for some diffeomorphism

$$s_2 = \phi(s_1), \text{ with } \phi'(s_1) > 0. \quad (1)$$

A diffeomorphic correspondence is useful when we expect the correspondence to be one-to-one. On the other hand, if there are substantial differences in shapes of the two curves, there may be segments of one curve whose shape cannot be found in the second curve. Topologically speaking, to match the two curves, we have to shrink these segments down to a point so that they disappear, and then rubber-sheet the result onto the second curve. This is illustrated in figure 1. The segment AB in C_1 has no corresponding segment in C_2, and the best way to match it to C_2 is to collapse it down to a point and map the collapsed point into C_2. Similarly, the segment CD in C_2 has a shape which cannot be found in C_1 and has to be collapsed before it can match to the point d in C_1. The resulting correspondence is not one-to-one.

An intuitive model for such correspondences can be constructed with the following procedure. We begin with two circles (two copies of S^1) and the *identity correspondence* between them. The identity correspondence pairs every point on the first circle with its copy on the second. Next, disconnected closed segments are marked on either circles (such as $A_1, A_2, \cdots$ in C_1 and $B_1, B_2 \cdots$ in C_2, fig 2a.) and each shrunk to a point (fig 2b) while continuously dragging the correspondence along (segments $A_k \in C_1$ are shrunk to points a_k and segments $B_k \in C_2$ are shrunk to points b_k). Now we have a correspondence between the two circles which models the creation and disappearance of segments. Continuing to drag the correspondence, one of the circles is distorted to give C_1 and the other to give C_2. The resulting correspondence models the disappearance and creation of segments in C_1 and C_2 (fig. 2c).

Next, we replace the intuitive acts of shrinking and distorting by functions. In figure 2, we think of the circles below Circle 1 and Circle 2 as entirely new circles and replace shrinking by functions q_1 and q_2. The function q_1 maps every point u of Circle 1 to the point on the circle below it where the original shrinking would have taken it. The function q_2 does the same for Circle 2. Intuitively, it is clear that q_1 and q_2 are continuous and differentiable functions from S^1 to S^1. Similarly, the distortion of the circles into C_1 and C_2 can be modeled with diffeomorphisms $h_1 : S^1 \to C_1$ and $h_2 : S^1 \to C_2$.

If (u, v) is an element of the original identity correspondence between Circle 1 and Circle 2, then the process of squeezing and distortion converts it to the element $(h_1 q_1(u), h_2 q_2(v))$ of the correspondence between C_1 and C_2. Using this development, we can clearly state the second model for correspondence.

Definition: Let S_1 and S_2 be two copies of S^1 and C_1 and C_2 be two curves diffeomorphic to S^1. A *bi-morphic correspondence* (or simply a *bi-morphism*) between C_1 and C_2 is the image of Φ_{id}, the identity correspondence between S_1 and S_2, under the map $\beta : S_1 \times S_2 \to C_1 \times C_2$ given by

$$\beta(u, v) = (h_1 q_1(u), h_2 q_2(v)),$$

for diffeomorphisms $h_1 : S^1 \to C_1$ and $h_2 : S^1 \to C_2$ and differentiable functions $q_1 : S^1 \to S^1$ and $q_2 : S^1 \to S^1$.

We call these correspondences bi-morphisms to suggest that they do not have a preferred direction (they are bi-directional) and that they "morph" the curves into each other. To additionally ensure that the bi-morphism is orientation preserving we impose the condition that q_1, q_2 and h_1, h_2 be orientation preserving functions.

The above definition gives bi-morphisms as sets. In fact, bi-morphisms have additional structure [9]:

Proposition 1: A bi-morphism is a closed curve in $C_1 \times C_2$.

The proposition is illustrated in fig. 3. The figure shows the curves C_1 and C_2. Their product space is a torus. Any element μ of a correspondence between the curves is a point on the torus. It pairs the point $p_1(\mu)$ on C_1 with the point $p_2(\mu)$ on C_2 (recall that p_1 and p_2 are projections). Proposition 1 states that a bi-morphism is in fact a curve on the torus. Figure 3 shows a specific correspondence as the curve containing μ.

Since any bi-morphism is a closed curve, it can be obtained as the image of a circle, i.e., any bi-morphism Φ can be written as $\Phi = \{(\phi_1^*(t), \phi_2^*(t))\}$, for functions $\phi_1^* : S^1 \to C_1 \times C_2$, and $\phi_2^* : S^1 \to C_1 \times C_2$. This is also shown in figure 3.

If L_1 and L_2 are the net arc-lengths of C_1 and C_2, and $\chi_1 : [0, L_1] \to C_1$ and $\chi_2 : [0, L_2] \to C_2$ are arc-length parametrization of C_1 and C_2, then the element $(\phi_1^*(t), \phi_2^*(t))$ of Φ pairs the point at arc-length $\chi_1^{-1}(\phi_1^*(t))$ on C_1 with the point at arc length $\chi_2^{-1}(\phi_2^*(t))$ on C_2 .

If we define $\phi_1(t) = \chi_1^{-1}\phi_1^*(t)$ and $\phi_2(t) = \chi_2^{-1}\phi_2^*(t)$, then an arc length can be obtained for the bi-morphism as $s = \int ds = \int_0^t \sqrt{\phi_1'^2(t) + \phi_2'^2(t)}\, dt$ [9].

The constraints that the bi-morphism is orientation preserving and arc-length parametrizable can be stated in terms of ϕ_1 and ϕ_2 as

$$\phi_1'(t) \geq 0, \ \phi_2'(t) \geq 0, \quad \text{and } \sqrt{\phi_1'^2(t) + \phi_2'^2(t)} > 0. \quad (2)$$

3 The Geometry of Non-rigid Shape Matching

The topological structure of bi-morphisms discussed above leads straight to the geometry of non-rigid curve matching. To proceed, we recall some definitions. Given a curve, if we choose a fixed unit circle

(the *Gaussian Circle*), then the outward normal at every point on the original curve can be translated so its base is at the center of the fixed circle. The *Gauss Map* is defined to be the map which takes each point of the curve to the tip of its translated vector on the Gaussian circle. Below, we denote the Gauss map by $\Theta(s)$, where Θ is the angular orientation of the normal at arc-length s. Its derivative with respect to arc-length is the curvature at s, $\kappa(s) = \frac{d\Theta(s)}{ds}$.

If $\mu(s)$ is an element of a bi-morphism Φ at arc length s along Φ, and $p_1(\mu(s))$ and $p_2(\mu(s))$ are its projections on C_1 and C_2, then the angular orientations of the normals at these points are $\Theta_1(p_1(\mu(s)))$ and $\Theta_2(p_2(\mu(s)))$.

The geometric criteria we propose is the following – since a bi-morphism is a curve, as μ moves along it, the derivatives of $\Theta_1(p_1(\mu(s)))$ and $\Theta_2(p_2(\mu(s)))$ with respect to the arc-length of Φ give the local shapes of C_1 and C_2 *as viewed from the bi-morphism.* The difference in the derivatives measures how closely the bi-morphism aligns the shapes of the curves.

The difference in the derivatives is

$$\frac{d\Theta_1(p_1(\mu(s)))}{ds} - \frac{d\Theta_2(p_2(\mu(s)))}{ds} = p_1'(\mu(s))\kappa_1(p_1(\mu(s))) - p_2'(\mu(s))\kappa_2(p_2(\mu(s))),$$

where, s is the arc-length along the bi-morphism.

Integrating the deviation of the above quantity from zero gives an index of dissimilarity of shapes of C_1 and C_2 as viewed from Φ. Denoting the index by $J(C_1, C_2; \Phi)$, we have

$$J(C_1, C_2; \Phi) = \int_\Phi \Gamma_1(\, p_1'(\mu(s))\kappa_1(p_1(\mu(s))) - p_2'(\mu(s))\kappa_2(p_2(\mu(s)))\,) \, ds,$$

where, Γ_1 is a non-negative function which measures the deviation of its argument from zero, $\Gamma_1() \geq 0$, and $\Gamma_1(x) = 0$ if and only if $x = 0$ (e.g. $\Gamma_1(x) = x^2$).

Using the definition of the arc-length of the bi-morphism, J can be expressed as

$$J(C_1, C_2; \phi_1, \phi_2) = \int_{S^1} \Gamma_1\Big(\frac{\phi_1'(t)\kappa_1(\phi_1(t)) - \phi_2'(t)\kappa_2(\phi_2(t))}{\sqrt{\phi_1'^2(t) + \phi_2'^2(t)}}\Big) \times \sqrt{\phi_1'^2(t) + \phi_2'^2(t)}\, dt. \quad (3)$$

The index J has three desirable properties: (1) It does not directly compare the numerical values of curvature, (2) It is symmetric with respect to C_1 and C_2, i.e. $J(C_1, C_2; \phi_1, \phi_2) = J(C_2, C_1; \phi_2, \phi_1)$, and (3) It is independent of any reparametrization of Φ. Thus, J compares the shapes of the curves while avoiding the problems associated with previous formulations.

We use J to compare similarity of shapes and choose the bi-morphism which gives the smallest value of J (subject to constraints of equation (2)) as the most desirable.

4 Exact Non-rigid Match

To gain further insight into comparison of shapes via non-rigid correspondence we explore conditions under which the two curves appear to be exactly matched, i.e. we seek conditions which make $J(C_1, C_2; \phi_1, \phi_2) = 0$. From equation (3) it follows that this is possible if and only if there is a bi-morphism Φ for which

$$\phi_1'(t)\kappa_1(\phi_1(t)) = \phi_2'(t)\kappa_2(\phi_2(t)). \quad (4)$$

The existence of such a bi-morphism is hard to establish in the general case. The investigation is much simpler if we impose the following technical constraints on the two curves:

(1) Their zeros of curvature occur only at a finite number of points,

(2) Their curvature is not a flat function at any of its zeros, i.e., if $\kappa(s_0) = 0$, then $\kappa^{(k+1)}(s_0) \neq 0$ for some k.

To analyze equation (4), we integrate it to get

$$\Theta_1(\phi_1(t)) - \Theta_1(\phi_1(0)) = \Theta_2(\phi_2(t)) - \Theta_2(\phi_2(0)), \quad (5)$$

which says that C_1 and C_2 can be exactly matched iff the Gauss map of C_1 viewed through ϕ_1 is a rotated copy of the Gauss map of C_2 viewed through ϕ_2.

To explore this further, recall that as a point moves clockwise over a convex segment of a curve (e.g., from u_1 to u_2 in the upper curve in figure 4) its image moves continuously and monotonically in a clockwise manner on the Gaussian circle (fig. 4). If the point moves clockwise over a concave segment (such as between u_2 and u_3 in figure 4) then its image through the Gauss map moves monotonically counter clockwise on the Gaussian circle. Hence, as the point traverses a convex segment and passes onto an adjoining concave segment (or conversely) its image on the Gaussian circle reverses direction. We call the point *on the Gaussian circle* at which this reversal happens a *fold point.* Clearly, a fold point is a local extremum of the Gauss map. Since the differential of the Gauss map is zero at local extrema, by our assumption, the Gauss maps of our curves have only a finite number of fold points.

Returning back to equation (5) recall that the Gauss maps of the two curves are identical except for a rotation. Suppose we rotate the Gauss map of the second curve through the required amount $(= \Theta_2(\phi_2(0)) - \Theta_1(\phi_1(0)))$, then the maps become identical; and in particular, their fold points coincide on the Gaussian circle.

Since ϕ_1 is continuous and orientation preserving, the fold points of $\Theta_1(\phi_1(t))$ on the Gaussian circle are identical to the fold points of $\Theta_1(s_1)$. Similarly, the fold points of $\Theta_2(\phi_2(t))$ on the Gaussian circle are identical to the fold points of $\Theta_2(s_2)$. Since the fold points of of $\Theta_1(\phi_1())$ and the rotated version of $\Theta_2(\phi_2())$ are identical, we conclude that the fold points of $\Theta_1()$ and the rotated version of $\Theta_2()$ are identical.

More precisely, suppose u_i, $i = 1, \cdots, N$ are points of C_1 whose images are successive fold points of its Gauss map, and v_j are points of C_2 whose images

are successive fold points of its Gauss map. Then the angular deviation $\Theta_1(u_{i+1}) - \Theta_1(u_i)$ between locations of successive fold points of C_1 on the Gaussian circle are identical to the angular deviation $\Theta_2(v_{\sigma(i+1)}) - \Theta_2(v_{\sigma(i)})$ for some circular shift $\sigma()$ of the index i, i.e., the strings

$$[\Theta_1(u_1) - \Theta_1(u_2), \Theta_1(u_2) - \Theta_1(u_3), \cdots, \Theta_1(u_N) - \Theta_1(u_1)]$$

and

$$[\Theta_2(v_{\sigma(1)}) - \Theta_2(v_{\sigma(2)}), \Theta_2(v_{\sigma(2)}) - \Theta_2(v_{\sigma(3)}), \cdots, \Theta_2(v_{\sigma(N)}) - \Theta_2(v_{\sigma(1)})]$$

are identical. We call these strings *angular deviation strings* since they tell us the angular deviation of the normal between the locations of successive fold points on the Gaussian circle.

Further analysis establishes the completeness of this result, that is [9] :

Proposition 2: A bi-morphism Φ satisfying equation (4) exists between two curves iff the curves have identical angular deviation strings (modulo circular shift).

Proposition 2 establishes an equivalence relation between curves. $C_1 \sim C_2$ if there exists a bi-morphism Φ for which $J(C_1, C_2; \phi_1, \phi_2) = 0$. From the proposition it follows that C_1 and C_2 have the same angular deviation strings, and hence $C_2 \sim C_1$. Finally, If $C_1 \sim C_2$ and $C_2 \sim C_3$, then all three of them have the same angular deviation strings and therefore $C_1 \sim C_3$.

Proposition 2 can be refined for diffeomorphic correspondences [9].

5 The Numerical Algorithm

When the two curves cannot be exactly matched, the optimal bi-morphism is found by seeking ϕ_1 and ϕ_2 that minimize J subject to constraints of equation (2). Since J is designed to be independent of any particular parametrization, a straightforward numerical minimization of J cannot uniquely determine ϕ_1 and ϕ_2. Numerical roundoff and data noise can cause the two functions to be unstable. To obtain stable performance, we regularize J by adding terms that depend on the smoothness of ϕ_1 and ϕ_2. The functional we minimize is

$$J_1(C_1, C_2; \phi_1, \phi_2) = J(C_1, C_2; \phi_1, \phi_2) + \zeta\left(\frac{L_1}{L_1 + L_2}\int_{S^1} \Gamma_2(\phi_1''(t))\, dt + \frac{L_2}{L_1 + L_2}\int_{S^1} \Gamma_2(\phi_2''(t))\, dt\right),$$

where, the first term is just the old index. The second term is the regularizing term with ζ being a small regularizing constant and $\Gamma_2()$ a positive function which (like $\Gamma_1()$) measures the deviation of its argument from zero. L_1 and L_2 are the total arc-lengths of C_1 and C_2 and are used to scale the relative contribution of C_1 and C_2 to regularization.

The most obvious choice for Γ_1 and Γ_2 is $\Gamma_1(x) = \frac{x^2}{\sigma_1^2}$ and $\Gamma_2(x) = \frac{x^2}{\sigma_2^2}$. However this choice is known to give an algorithm sensitive to outliers in the data [2]. Instead we choose functions which behave like x^2 for small values of x and are robust against outliers. We use [2]

$$\Gamma_1(x) = \lg(1 + \frac{x^2}{\sigma_1^2}), \quad \text{and} \quad \Gamma_2(x) = \lg(1 + \frac{x^2}{\sigma_2^2}).$$

In the numerical algorithm we approximate ϕ_1 and ϕ_2 as piece-wise linear functions and use a discrete version of projected gradient descent to obtain the optimal correspondence. Each curve is sampled uniformly at N points along its arc-length, giving an $N \times N$ grid in $C_1 \times C_2$ (fig. 5). The circle S^1 is sampled at M knot points t_i, $i = 1, \cdot, M$. The functions ϕ_1 and ϕ_2 are piece-wise linear between consecutive knot points, hence they are completely determined by their value at the knot points. The functions are further constrained so that the knot $(\phi_1(t_i), \phi_2(t_i))$ can only be one of the $N \times N$ grid points. In other words, the correspondence is an M-sided polygon in $C_1 \times C_2$ whose vertices are some subset of the $N \times N$ grid points.

The optimization algorithm has two stages: in the first stage a good initial guess of ϕ_1 and ϕ_2 is obtained, and in the second stage the guess is iteratively improved by locally descending in the solution set defined by equation (2). The initial guess is obtained by starting from several correspondences that uniformly map the arc-length of C_1 to the arc-length of C_2, executing one iteration of the descent, and choosing the result which has the smallest value of J_1. Further details of the algorithm are available in [9]. The values of N, M, ζ, σ_1 and σ_2 used in the algorithm are shown in Table 1.

Symbol	Name	Value
N	Mesh Points on each Curve	120
M	Knot Points for Bi-mophism	10
ζ	Regularization Constant	9.0
σ_1		40.0
σ_2		25.0

Table 1. Constants Used in Numerical Experiments.

6 Experiments

Due to lack of space we cannot exhibit all experimental results. We present some examples from real-world images. Additional examples can be found in [9].

Figures 6 and 7 are MRI images of a dog heart. obtained at diastole and systole. The endocardium (inside of the left ventricular cavity) is outlined by hand in both images. Figure 8 shows the two curves overlaid in the same image (magnified for better viewing) and the bi-morphism found by the algorithm of the previous section. The bi-morphism matches the shape features well; in particular, the papillary muscles (the triangular notches at 2 and 8 o'clock) are matched well. The correspondence provides some indication of the non-rigid motion of the heart.

Figures 9 and 10 show the initial and final images of the growth cone lamellipodium of an Aplysia neuron with the outlines drawn on the image. Figure 11 shows the bi-morphism found by the algorithm. The bi-morphism strongly suggests the temporal development of shape of the growth cone.

7 Conclusion

We proposed a geometric procedure for non-rigid shape-based correspondence between curves. It is free of the problems of earlier procedures. We also analyzed curves whose shape can be exactly matched and showed that these curves form equivalence classes. Experiments with real-world data indicate that the technique can be used in a number of applications.

Acknowledgements

This research was supported by the grant LM05007-04 from the N.L.M. and the grant DMS 9404497 from the N.S.F.

References

[1] Cohen I., Ayache N. Sulger P., "Tracking Points on Deformable Objects Using Curvature Information," Vol. 588, Lecture Notes in Computer Science: ECCV '92. Springer-Verlag, Berlin, 1992.

[2] Black M., Rangarajan A., "The Outlier Process: Unifying Line Processes and Robust Statistics," IEEE Conf. CVPR, 1994.

[3] Duncan J. S., Owen R. L., et al., "Measurement of Non-Rigid Motion Using Contour Shape Descriptors," Proc. CVPR, Maui, HI, 1991, 318-324.

[4] Feldman J., Ayache N., "Locally Affine Registration of Free-form Surfaces," Proc. CVPR 1994, Seattle, WA, 496-501.

[5] Gold S., Lu C. P., Rangarajan A., et al., "New Algorithms for 2D and 3D Point Matching: Pose Estimation and Correspondence," Advances in Neural Inf. Proc. Sys., 7, 1995. (to appear)

[6] Kambhamettu C., Goldgof D., "Point Correspondence Recovery in Non-rigid Motion," Proc. CVPR, 1992, 222-227.

[7] McEachen J. C., Duncan J. S., "A Constrained Analytic Solution for Tracking Non-rigid Motion of the Left Ventricle," IEEE 18th Annual Northeast Bioengineering Conf., Univ. of Rhode Island, March 1992, 137-138.

[8] Pelizarri C., Chen G., et al., "Accurate Three-dimensional Registration of CT, PET, and/or MR Images of the brain," J. Computer Assisted Tomography, 13(1):20-26, 1989.

[9] Tagare H. D., O'Shea D., "The Topology and Geometry of Non-rigid Shape-based Correspondence," Technical Report, *Forthcoming*.

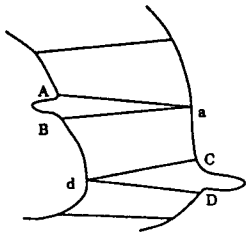

Figure 1: Pairing Segments with Points.

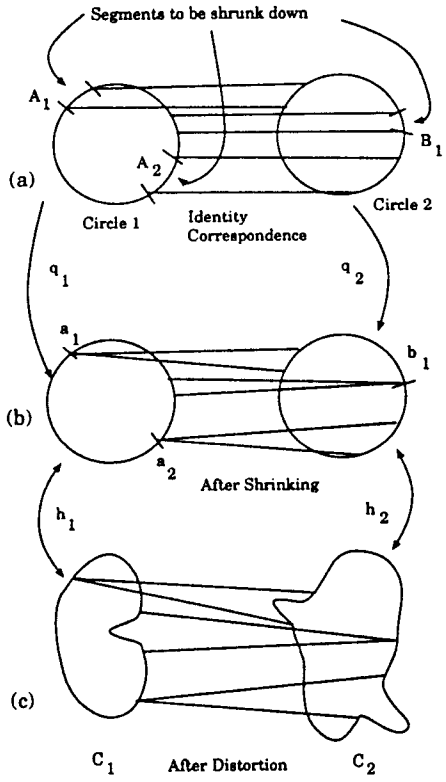

Figure 2: Bi-morphic Correspondence.

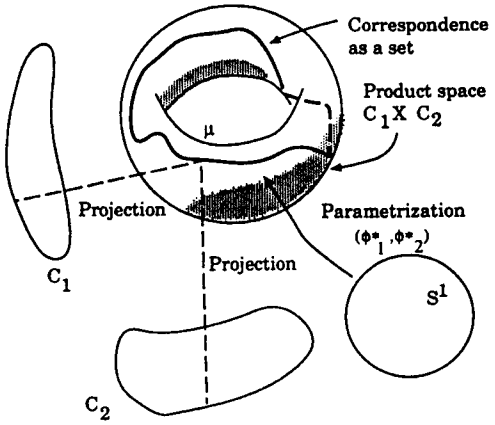

Figure 3: Structure of a Bi-morphism.

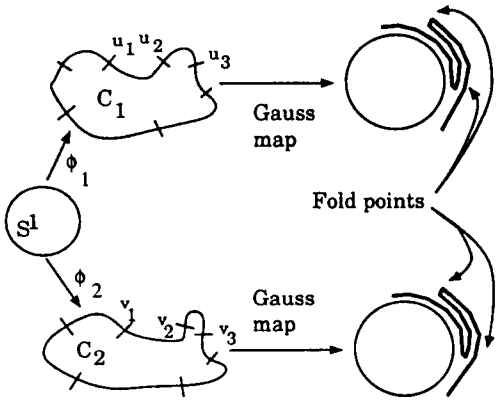

Figure 4: Folds of the Gauss Map.

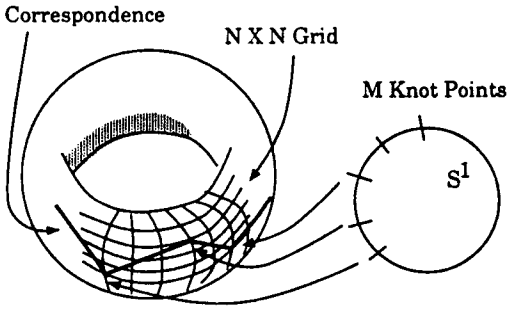

Figure 5: Discretization.

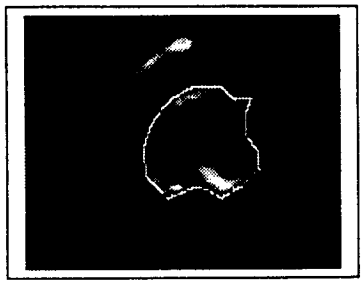

Figure 6: Short Axis view at Diastole.

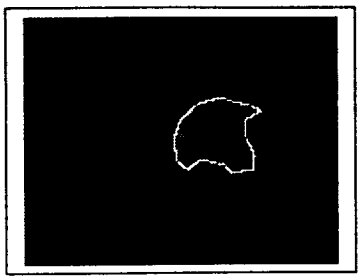

Figure 7: Short Axis view at Systole.

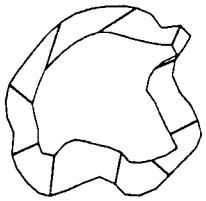

Figure 8: Correspondence between Endocardium Outlines.

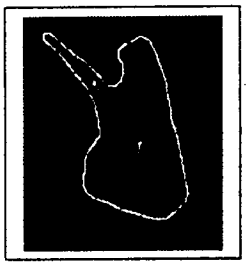

Figure 9: Growth Cone - Initial Image.

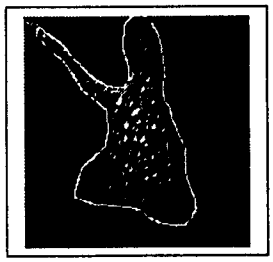

Figure 10: Growth Cone - Final Image.

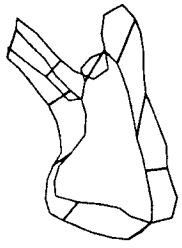

Figure 11: Correspondence between Outlines.